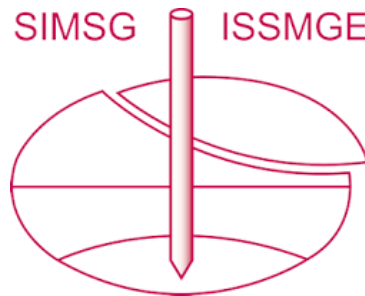


INTERNATIONAL SOCIETY FOR SOIL MECHANICS AND GEOTECHNICAL ENGINEERING



This paper was downloaded from the Online Library of the International Society for Soil Mechanics and Geotechnical Engineering (ISSMGE). The library is available here:

<https://www.issmge.org/publications/online-library>

This is an open-access database that archives thousands of papers published under the Auspices of the ISSMGE and maintained by the Innovation and Development Committee of ISSMGE.

The paper was published in the proceedings of the 7th International Conference on Earthquake Geotechnical Engineering and was edited by Francesco Silvestri, Nicola Moraci and Susanna Antonielli. The conference was held in Rome, Italy, 17 - 20 June 2019.

Ground motion scaling for the assessment of the seismic response of a diaphragm wall

G. Elia & A. di Lernia

Department of Civil, Environmental, Land, Building Engineering and Chemistry (DICATECh), Politecnico di Bari, Italy

M. Rouainia

School of Engineering, Newcastle University, UK

ABSTRACT: Nonlinear finite element analysis represents an advanced numerical approach to study the dynamic performance of geotechnical structures subjected to earthquakes. The approach requires the use of sophisticated soil constitutive assumptions and the correct definition of the bedrock input motions, opportunely selected to be representative of the site seismic hazard. Different input motion scaling methods have been proposed to minimise the bias and reduce the number of simulations needed to obtain statistically stable and robust results. These scaling methods have mainly been adopted in structural engineering, but their application in geotechnical earthquake engineering problems is still limited. The paper investigates the effect of five different earthquake scaling/matching strategies on the nonlinear dynamic response of an anchored diaphragm wall supporting a deep excavation in Boston Blue Clay. Two seismic intensity levels are considered. The results are interpreted, for each scaling/matching technique, in terms of seismic induced maximum horizontal displacements of the wall.

1 INTRODUCTION

It is well recognised that the nonlinear finite element (FE) analysis is a sophisticated tool to investigate the performance of geotechnical structures subjected to earthquake loading. It has the ability to consider complex conditions in terms of heterogeneity of soil strata and to account for the interaction between the soil deposit and sub-surface structures, such as tunnels and retaining systems. On the other hand, the approach requires the use of advanced soil constitutive relationships and the correct definition of the bedrock input motions, selected according to the seismic hazard of the site.

In the earthquake geotechnical engineering field, the seismic input signals are typically scaled to the PGA (Peak Ground Acceleration) of the specific site, representing the maximum acceleration expected at the bedrock outcropping surface. Nevertheless, different ground motion modification methods might be used to modify the selected acceleration time histories, in order to minimise the bias and reduce the number of simulations needed to obtain statistically stable and robust results. In fact, the input motion might be linearly scaled by using a suitable Scale Factor (SF) without altering the shape of the response spectrum or modified in its spectral shape by adding wavelets to match a target spectrum. Whereas the adoption of such scaling/matching techniques is common in the structural engineering literature (e.g. Shome et al. 1998; Hancock et al. 2006; Haselton 2009; Galasso 2010; Michaud and Léger 2014), their application to geotechnical earthquake engineering problems is still limited (e.g. Amirzehni et al. 2015; Guzel et al. 2017).

The present work investigates the effect of five different earthquake scaling/matching strategies on the dynamic response of an anchored diaphragm wall supporting a deep excavation in Boston, USA. The excavation phase and the installation of the diaphragm wall under static

conditions has been studied by Rouainia et al. (2017). The retaining structure mainly interacts with a thick layer of Boston Blue Clay (BBC), whose mechanical behaviour can be successfully described using the advanced constitutive model for natural clays developed in the framework of kinematic hardening plasticity by Rouainia and Muir Wood (2000), enhanced to account for the variation of the shear stiffness modulus with mean effective stress and overconsolidation ratio (OCR). The selected seismic input motions are here linearly scaled according to PGA, $S_a(T_1)$, ASCE and MSE scaling methods or modified to match the target spectrum using the Spectral Matching technique. Two seismic intensity levels are investigated in the nonlinear FE analyses of the diaphragm wall. The results are interpreted, for each scaling/matching technique, in terms of maximum horizontal displacement of the wall induced by each earthquake. This allows the best scaling/matching strategy to be identified from a statistical point of view, leading to smallest variability in the results depending on the intensity level considered in the analysis.

2 NUMERICAL MODEL

The dynamic performance of the excavation and supporting diaphragm wall is investigated through 2D nonlinear FE analyses performed with PLAXIS 2D (Brinkgreve et al. 2016). The problem refers to the case study of a 14.6 m deep, 100 m wide basement excavation for the Allston Science Complex located in Boston, Massachusetts (Buro Happold 2017). The local geological profile is characterised by a 2 m thick layer of made ground (L1), overlaying a 4 m stratum of fluvial sand (L2), followed by a 26 m deep Boston Blue Clay layer (L3) and 8 m of glacial till (L4), resting on Cambridge argillite bedrock. The water table is located at a depth of 2 m below the ground surface. A detailed description of the geotechnical characterization of the site is reported in Rouainia et al. (2017).

The 2D plane strain FE mesh consists of 7439, 15-noded triangular elements and 60669 nodes. The geometrical model is 40 m deep and 420 m wide, where the lateral sides are set far enough to avoid any interference of the vertical boundaries with the area of interest. The excavation is retained by a 21 m diaphragm wall with four rows of tieback anchors. For the sake of convenience, only half of the model is reported in Figure 1. The diaphragm wall is modelled with elastic plate elements, characterised by unit weight equal to 22 kN/m^3 , normal stiffness EA equal to $2.28 \times 10^7 \text{ kN/m}$ and flexural rigidity EI equal to $1.59 \times 10^6 \text{ kNm}^2/\text{m}$. The anchors are modelled as elasto-plastic elements characterised by a normal stiffness of $1.12 \times 10^5 \text{ kN/m}$ and a pre-stress force of 383 kN/m. The interaction between the retaining structure and the soil layers is modelled by means of interface elements, assuming a soil-wall friction angle equal to $2/3$ of the friction angle of the surrounding soil layers. Particular attention is given to the size of the finite elements, which are smaller than one-eighth of the wavelength associated with the maximum frequency of the signals, in order to prevent from filtering their high frequencies.

The FE simulation involves a first static stage, followed by a dynamic analysis. The static stage simulates the excavation and the installation of the retaining structure. The construction sequence consists in the installation of the retaining wall, followed by a first excavation phase under cantilever conditions and then tiebacks installation and consecutive excavation to 0.6 m below each level of the tiebacks. Once the last tieback is installed, then the final excavation to

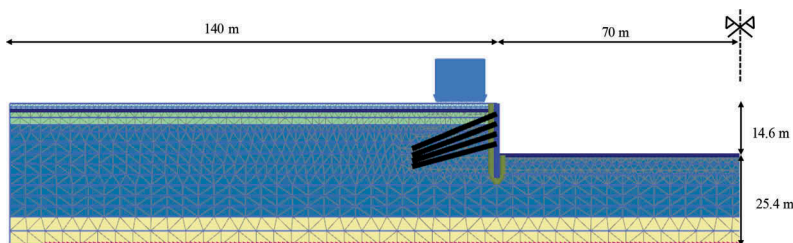


Figure 1. FE model adopted in PLAXIS - end of the excavation

14.6 m is simulated and the earthquake is supposed to take place after this final phase. The static stages as well as the dynamic analyses are performed under undrained conditions. Total fixities at the bottom of the mesh and lateral sides free to move only in the vertical direction are used to represent the static boundary conditions. During the dynamic stage, tied-nodes lateral boundary conditions are adopted, while the input motions are directly applied at the base of the model as displacement time histories.

The made ground (L1), fluvial sand (L2) and glacial till (L4) strata are modelled with the elastic-perfectly plastic Mohr-Coulomb (MC) model, while the BBC behaviour is described by the RMW model proposed by Rouainia and Muir Wood (2000) and recently validated under cyclic and dynamic loading conditions (Elia and Rouainia 2016; Elia et al. 2017; Cabangon et al. 2018). The local soil profile is presented in Figure 2a. RMW is characterised by three surfaces: the reference surface, controlling the state of the reconstituted structureless soil, the structure surface, representing the amount of structure of the natural clay, and the bubble, enclosing the elastic domain. The elastic response of the model is governed by the elastic formulation proposed by Viggiani and Atkinson (1995), for which the small-strain shear modulus is nonlinearly dependent on the mean effective stress and the OCR.

The calibration of the RMW parameters is described in detail by Rouainia et al. (2017) and their values are reported in Table 1. The BBC layer is herein assumed to be characterised by an OCR constant with depth and equal to 1.75. According to the calibrated parameters, the elastic response of the BBC soil is represented by the small-strain shear stiffness G_0 profile illustrated in Figure 2b, while the cyclic response is described by the shear stiffness modulus and damping ratio curves shown in Figure 2c.

The mechanical properties for the MC layers under static conditions, derived from geotechnical reports on Boston soils, are reported in Table 2. The dynamic response of these soils is, instead, described by material parameters compatible with the average shear strain induced by the earthquakes. Thus, preliminary equivalent linear simulations are performed with EERA (Bardet et al. 2000), adopting the normalised shear modulus and damping curves and the initial stiffness profile (G_0) shown in Figure 2. The calibration of the dynamic properties of the MC soil layers is carried out using the acceleration time histories of seven earthquakes scaled to the PGA of the site, equal to 0.058g for low and 0.35g for high intensity events. The profiles of shear stiffness and damping ratio obtained for each earthquake are illustrated in Figure 3. The MC dynamic parameters adopted in the FE simulations are, therefore, obtained from the average of the preliminary equivalent linear analyses results for each soil layer.

Table 1. RMW parameters for the BBC soil layer

M	λ^*	κ^*	R	B	ψ	η_0	r_0	A^*	k	ν
1.11	0.028	0.004	0.08	2.0	1.35	0	1.5	0.5	1.0	0.25

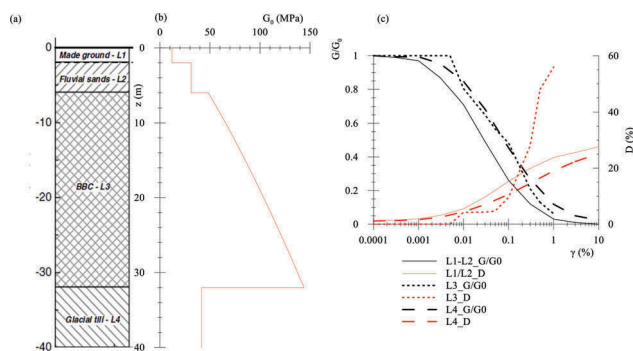


Figure 2. Local soil profile: (a) soil stratigraphy, (b) initial shear stiffness profile, (c) normalised shear modulus and damping ratio curves

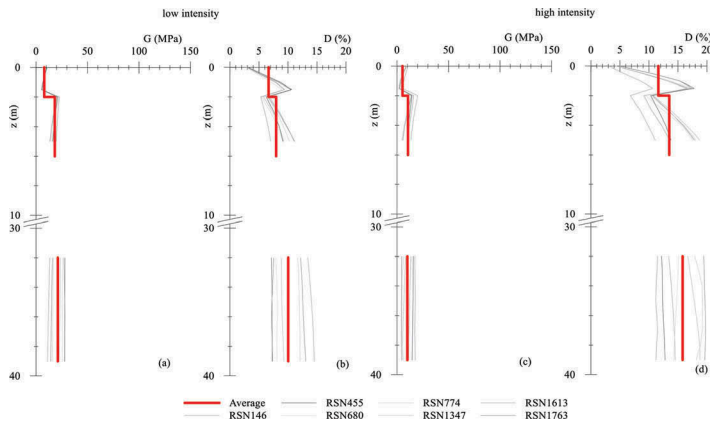


Figure 3. Calibration of the shear stiffness and damping ratio profiles based on equivalent linear analyses

Table 2. Material parameters of the MC soil layers

Layer	Depth m	γ kN/m ³	ϕ' °	K_0 -	E' kPa	ν -	G_0 MPa
L1	0 – 2	19.0	30	0.50	29	0.20	12.08
L2	2 – 6	19.0	35	0.43	75	0.20	31.25
L4	32 – 40	21.5	37	0.40	100	0.20	41.67

Table 3. Dynamic parameters calibrated for low and high intensity levels

Layer	low intensity				high intensity			
	G MPa	Rayleigh D %	α_R -	β_R -	G MPa	Rayleigh D %	α_R -	β_R -
L1	7.999	6.66	0.65577	0.001954	5.35	11.62	1.14407	0.003409
L2	18.21	7.96	0.78386	0.002336	10.64	13.50	1.32912	0.003960
L3	$f(\gamma\%)$	1.00	0.09845	0.000293	$f(\gamma\%)$	1.00	0.09845	0.000293
L4	21.14	10.04	0.98873	0.002946	10.05	15.80	1.55567	0.004636

For the MC layers, the material damping is introduced by means of the Rayleigh formulation, which requires an adequate calibration strategy for the definition of the control frequencies. The Rayleigh coefficients α_R and β_R are evaluated assuming control frequencies f_m and f_n equal to 0.85 Hz and 10 Hz, respectively, for all the simulations. The first control frequency f_m is identified as the average value of the first natural frequency of the soil deposit obtained by preliminary equivalent linear analyses, while the value of 10 Hz is selected, regardless the content of each applied input motion, to be sufficiently high to cover a wide frequency range. For the BBC layer, only 1% of viscous damping is added to provide dissipation at very small-strain levels. The resulting values of G and D adopted in the dynamic simulations performed with PLAXIS are summarised in Table 3 along with the Rayleigh damping parameters used to introduce viscous damping in the FE analyses.

3 INPUT MOTION SCALING METHODS

Following the recommendation of the NEHRP provisions (NEHRP 2015), nonlinear FE dynamic analyses of the excavation are performed using seven earthquakes, selected from the

Table 4. Selected input motions

Earthquake Name	RSN	Date	Magnitude	Durations
Coyote Lake	146	06/08/1979	5.74	26.85
Morgan Hill	455	24/04/1984	6.19	29.99
Whittier Narrows-01	680	01/10/1987	5.99	39.99
Loma Prieta	774	18/10/1989	6.93	39.43
Chi-Chi	1347	20/09/1999	7.62	78.99
Duzce	1613	12/11/1999	7.14	43.98
Hector Mine	1763	16/10/1999	7.13	43.99

PEER database (Ancheta et al. 2013). The selection is based on the best fitting of the target response spectrum, obtained as a result of the seismic hazard of the Boston site. Specifically, the seismic hazard analysis reveals that Boston is characterised by a low-medium seismicity, with a predicted PGA at bedrock equal to 0.058g. The selected seismic motions are summarised in Table 4.

With the aim of being representative of the seismic demand of the site, each input motion can be modified through linear scaling procedures, consisting in scaling the accelerogram without altering its spectral shape, or spectral matching, requiring the addition and subtraction of wavelets to the original signal in the time domain in order to obtain a modified signal, whose response spectrum matches the target one. The limits of these scaling procedures are discussed in a number of previous works (e.g. Vanmarcke 1979; Bommer and Acevedo 2004; Huang et al. 2011). In this paper, five scaling/matching methods are adopted to modify the input motions, specifically the PGA, $S_a(T_1)$, ASCE and MSE scaling techniques and the Spectral Matching (SM) method. In detail, the PGA scaling technique consists in multiplying the acceleration time history by a scale factor determined such that the PGA of the scaled motion is equal to the target PGA. In the $S_a(T_1)$ scaling method the SF is evaluated such that the spectral acceleration of each record at the fundamental period of the system T_1 is the same as the one of the target spectrum at the same period. Thus, the determination of the fundamental period of the system plays a major role in this technique. Herein, T_1 is assumed equal to the elastic period of the free-field soil deposit (i.e. $T_1 = 0.88s$), evaluated as a function of its thickness, i.e. 40 m, and an average shear wave velocity $V_{s,30}$ equal to 183 m/s. According to the ASCE provisions (ASCE 2010), the ground motions should be scaled such that the average response spectrum of the scaled records is not smaller than the target response spectrum over the fixed range of periods between $0.2T_1$ and $1.5T_1$. Finally, the MSE scaling technique consists in scaling the acceleration time histories in a way that the mean square error between the target spectrum and the average response spectrum is minimum within a defined period range, assumed here equal to 0.1 - 2s. The Spectral Matching of the input motions is, instead, achieved using the computer program SeismoMatch (Seismosoft 2016). The program allows to modify the recorded acceleration time histories to obtain a response spectrum very close to the target one in a predefined period range, assumed in this case equal to 0.02 - 2s.

To investigate the performance of the excavation in an ideal scenario of high seismicity, the high intensity level motions are here obtained by simply scaling the target spectrum to a PGA equal to 0.35g. Therefore, the same low intensity signals previously selected from the database are just multiplied by higher scale factors to obtain the corresponding high intensity level motions matching the new target spectrum. The resulting scale factors for low and high intensity level associated to each scaling method are summarised in Table 5. The spectrally matched input motions at high intensity are obtained by multiplying the spectrally matched low intensity motions by a SF of 4.644. The average response spectra obtained by each scaling/matching technique are compared to the target response spectrum in Figure 4 for the low intensity case only. After being scaled or spectrally matched, the input motions are baseline corrected and filtered with a low-pass Butterworth filter with cut-off frequencies higher than 20 Hz.

Table 5. Scale factors adopted for each scaling techniques for low and high intensity levels

RSN	low intensity				high intensity			
	MSE	PGA	$S_a(T_1)$	ASCE	MSE	PGA	$S_a(T_1)$	ASCE
146	0.862	0.7972	0.7639	0.7	4.003	3.702	3.547	3.250
455	0.9824	1.0725	1.0744	1.2	4.562	4.980	4.989	5.572
680	0.5744	0.6709	0.4674	0.55	2.667	3.115	2.170	2.554
774	0.9619	1.5366	0.7583	1.5	4.467	7.135	3.521	6.965
1347	0.6554	0.7944	0.9345	0.9	3.043	3.689	4.339	4.179
1613	1.4225	2.933	1.0513	1.8	6.605	13.619	4.882	8.358
1763	1.2264	2.1161	0.8861	1.5	5.695	9.826	4.115	6.965

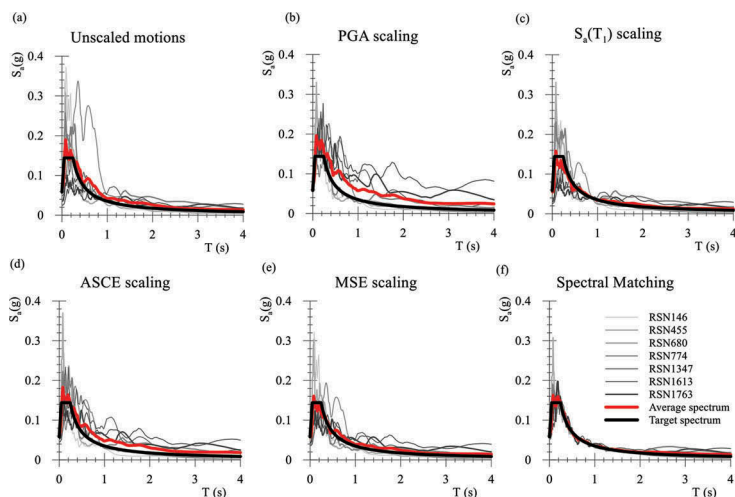


Figure 4. Input motion response spectra for the low intensity case: (a) unscaled records, (b) PGA scaling, (c) $S_a(T_1)$ scaling, (d) ASCE scaling, (e) MSE scaling and (f) Spectral Matching

4 NUMERICAL RESULTS

The numerical results, for both low and high intensity levels, are illustrated in Figure 5 in terms of maximum horizontal displacement of the diaphragm wall obtained at the end of the dynamic simulations. For each scaling/matching technique, the mean value of the maximum displacement is evaluated, together with the standard deviation (σ) representing a measure of the FE results scattering around the mean. With reference to low intensity earthquakes, the mean horizontal displacement computed for each strategy ranges between 2 and 5 cm. The best performance in terms of reduced variability of the wall displacement around the mean is provided by the $S_a(T_1)$ scaling and SM methods. The most commonly used scaling techniques (i.e. PGA and ASCE scaling) do not return good statistical results, while the MSE scaling method is characterised by a mean displacement close to that obtained with the $S_a(T_1)$ and SM techniques, but provides a higher dispersion of the results. The same trend can be detected with reference to the high intensity level analyses, for which $S_a(T_1)$, MSE and SM are characterised by about the same mean displacement value. However, the SM method gives the smaller response variability in terms of standard deviation, while MSE and $S_a(T_1)$ are characterised by a higher dispersion of the results. Again, the most common PGA and ASCE scaling techniques provide the worst performance from a statistical point of view. For the high intensity level, the mean horizontal displacement of the diaphragm wall oscillates between 10 and 55 cm. The

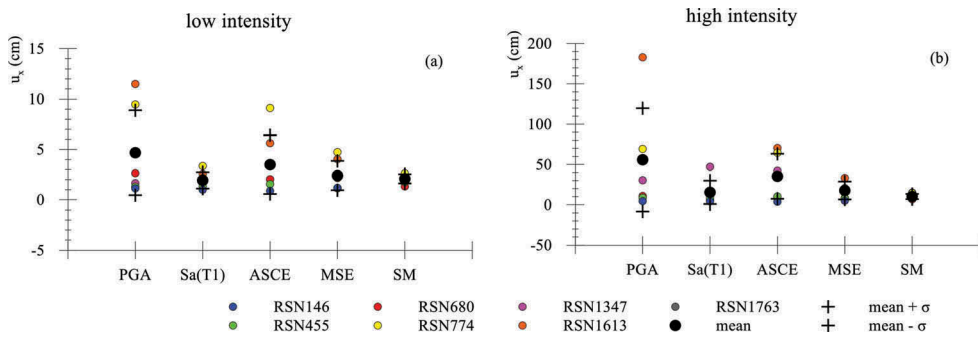


Figure 5. Maximum horizontal displacement of the wall obtained with the different scaling/matching techniques: (a) low intensity, (b) high intensity case

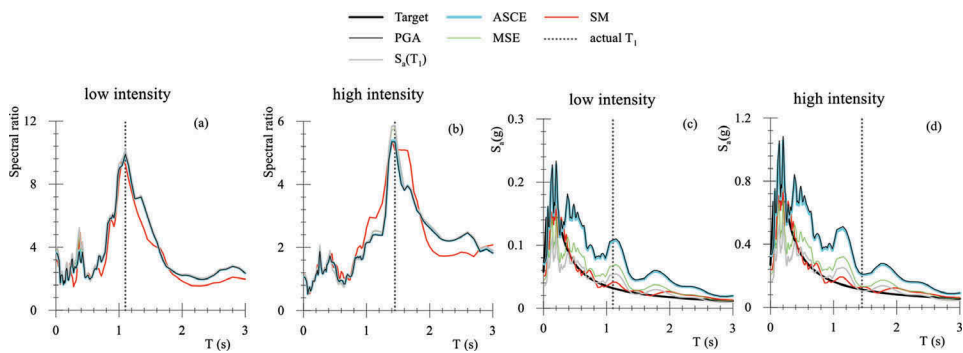


Figure 6. Amplification function of the RSN774 signal for the (a) low intensity, (b) high intensity case. Response spectra of the RSN774 input motion for the (c) low intensity, (d) high intensity case

obtained results can be justified observing the amplitude of the bedrock motion around the first period of oscillation of the system composed by the diaphragm wall and the surrounding soil deposit. It should be highlighted that the fundamental period of the system elongates from the free-field value (i.e. T_1) to a greater value, depending on the level of soil nonlinearity induced during the wave propagation process and soil-structure interaction. In particular, for low intensity earthquakes the first natural period of the system increases to 1.1s, while it becomes equal to 1.45s for high intensity signals, as can be detected from the amplification functions shown in Figure 6a and b for one of the seven earthquakes (i.e. RSN774). Consequently, the wave propagation process is dominated by the magnitude that the spectral acceleration of the input motion attains around the first natural period of the system (Figure 6c and d). This, in turn, explains why the smallest variability of the output is obtained by applying the $S_a(T_1)$ and SM techniques for low intensity motions, and MSE and SM for high intensity motions. In fact, scaling the earthquake with the various techniques, the spectral accelerations at bedrock attain very different values around the fundamental period of the system, higher for PGA and ASCE scaling and decreasing for MSE, $S_a(T_1)$ and SM, consistently with the pattern of the maximum displacement of the wall shown in Figure 5.

5 CONCLUSIONS

The paper presents a numerical study on the influence of the input motion scaling/matching methods on the dynamic response of a diaphragm wall. The numerical investigation refers to

the case study of a deep excavation in Boston. Five scaling/matching techniques are chosen to linearly or spectrally modify seven input motions, selected on the basis of the seismic hazard analysis of the site. The results of the nonlinear dynamic simulations are illustrated in terms of mean and standard deviation of the maximum horizontal displacement experienced by the wall during each set of input motions. The work highlights the importance of the strategy adopted to scale/match the bedrock motions in reducing the level of variability of the dynamic response of a typical soil retaining structure. The results of the statistical analysis indicate that, for low intensity input motions, the $S_a(T_1)$ scaling and spectral matching methods are characterised by the lowest mean and standard deviation of the output, while higher variability is obtained using the MSE, ASCE and PGA scaling techniques. When higher seismic intensity levels are considered, the best performance is provided by the MSE scaling and SM techniques.

REFERENCES

- Amirzehni, E., Taiebat, M., Finn, W.D.L. & Devall, R.H. 2015. Ground Motion Scaling/matching for Nonlinear Dynamic Analysis of Basement Walls. In *The 11th Canadian Conference on Earthquake Engineering*. Victoria, BC, Canada.
- Ancheta, T.D., Darragh, R.B., Stewart, J.P., Seyhan, E., Silva, W.J., Chiou, B.S.J., Wooddell, K.E. 2013. *PEER NGA-West2 Database*, PEER Report 2013/03. Berkley.
- ASCE. 2010. *ASCE/SEI 7-10: Minimum Design Loads for Buildings and Other Structures*. Reston, VA.
- Bardet, J.P., Ichii, K. & Lin, C.H. 2000. *EERA: A Computer Program for Equivalent-Linear Earthquake Site Response Analyses of Layered Soil Deposits*. University of Southern California, Berkley.
- Bommer, J.J. & Acevedo, A.B. 2004. The Use of Real Earthquake Accelerograms as Input to Dynamic Analysis. *Journal of Earthquake Engineering* 8 (S1): 43–91.
- Brinkgreve, R.B.J., Kumarswamy, S. & Swilfs, W.M. 2016. *PLAXIS 2D 2016*. Reference Manual. Delft, The Netherlands.
- Buro Happold. 2007. *Harvard Allston Science Complex. Geotechnical Report Revision 4*. Bath, UK.
- Cabangon, L.T., Elia, G. & Rouainia, M. 2018. Modelling the Transverse Behaviour of Circular Tunnels in Structured Clayey Soils during Earthquakes. *Acta Geotechnica* (in print).
- Elia, G. & Rouainia, M. 2016. Investigating the Cyclic Behaviour of Clays Using a Kinematic Hardening Soil Model. *Soil Dynamics and Earthquake Engineering* 88: 399–411.
- Elia, G., Rouainia, M., Karofyllakis, D. & Guzel, Y. 2017. Modelling the Non-Linear Site Response at the LSST down-Hole Accelerometer Array in Lotung. *Soil Dynamics and Earthquake Engineering* 102: 1–14.
- Galasso, C. 2010. *Consolidating Record Selection for Earthquake Resistant Structural Design*. PhD Thesis. Università degli Studi di Napoli “Federico II”.
- Guzel, Y., Elia, G. & Rouainia, M. 2017. The Effect of Input Motion Selection Strategies on Nonlinear Ground Response Predictions. In *COMPdyn 2017-6th International Thematic Conference*. Rhodes Island (GR): National Technical University of Athens.
- Hancock, J., Watson-Lamprey, J., Abrahamson, N.A., Bommer, J.J., Markatis, A., McCoyh, E. & Mendis, R. 2006. An Improved Method of Matching Response Spectra of Recorded Earthquake Ground Motion Using Wavelets. *Journal of Earthquake Engineering* 10 (sup001): 67–89.
- Haselton, C.B. 2009. *Evaluation of Ground Motion Selection and Modification Methods: Predicting Median Intersory Drift Response of Buildings*. PEER Report. Berkeley.
- Huang, Y.-N., Whittaker, A.S., Luco, N. & Hamburger, R.O. 2011. Scaling Earthquake Ground Motions for Performance-Based Assessment of Buildings. *Journal of Structural Engineering* 137 (3): 311–321.
- Michaud, D. & Léger, P. 2014. Ground Motions Selection and Scaling for Nonlinear Dynamic Analysis of Structures Located in Eastern North America. *Canadian Journal of Civil Engineering* 41 (3): 232–244.
- NEHRP. 2015. *NEHRP Recommended Seismic Provisions for New Buildings and Other Structures*. Washington.
- Rouainia, M. & Muir Wood, D. 2000. A Kinematic Hardening Constitutive Model for Natural Clays with Loss of Structure. *Geotechnique* 50 (2): 153–164.
- Rouainia, M., Elia, G., Panayides, S. & Scott, P. 2017. Nonlinear Finite-Element Prediction of the Performance of a Deep Excavation in Boston Blue Clay. *Journal of Geotechnical and Geoenvironmental Engineering* 143 (5): 04017005.
- Seismosoft. 2016. *SeismoMatch - A Computer Program for Spectrum Matching of Earthquake Records*.

- Shome, N., Cornell, C.A., Bazzurro, P. & Carballo, J.E. 1998. Earthquakes, Records, and Nonlinear Responses. *Earthquake Spectra* 14 (3): 469–500.
- Vanmarcke, E.H. 1979. Representation of Earthquake Ground Motion: Scaled Accelerograms and Equivalent Response Spectra. *State-of-the-Art for Assessing Earthquake Hazards in the United States, Report 14, Miscellaneous Paper S-73-1*. US Army Corps of Engineers, Vicksburg, Mississippi.
- Viggiani, G. & Atkinson, J.H. 1995. Stiffness of Fine-Grained Soil at Very Small Strains. *Geotechnique* 45 (2): 249–265